Sensors & Diagnostics

PAPER

View Article Online
View Journal | View Issue

Cite this: *Sens. Diagn.*, 2022, **1**, 1189

Optical detection of pH changes in artificial sweat using near-infrared fluorescent nanomaterials†

Nigar Sultana, Hannah Dewey and Januka Budhathoki-Uprety *

Increasing demand for pH measurements for healthcare, food safety, environmental monitoring, and industrial treatments require molecular probes and sensors capable of measuring pH in specific environments. In biological systems, pH changes in tissues and biofluids including urine, sweat, and blood could indicate patho-physiological conditions such as tumor metastasis, microbial infection, acidosis, cystic fibrosis, wound healing, *etc.* Sweat analysis provides a non-invasive and convenient measure to monitor personal health. Thus, monitoring sweat pH could provide insights on patho-physiological changes. Optical pH measurements have gained significant interest in recent decades due to versatile material choices and new imaging technologies that allow exciting new applications. Single-walled carbon nanotubes (SWCNTs) are emerging molecular optical probes and sensors because of their outstanding photophysical properties, which include fluorescence in the near-infrared (nIR) spectral range, sensitivity to the molecular recognition, and non-photo bleaching nIR emission. Tunable surface functionalization on SWCNTs could produce targeted molecular probes that are responsive to environmental clues including changes in solution pH. This research describes the development of SWCNT-based optical probes to enable detection of pH changes in aqueous media and artificial sweat as a model biofluid. The sensors can reliably detect pH changes within a biologically relevant range and beyond, through changes in nIR emission. The sensors that can respond within this pH range are valuable investigational tools in certain disease conditions that experience extreme pH changes. We modulated the surface chemistry of nanotubes with a polymer and showed that the sensor response direction can be modulated upon surface chemistry changes (for example, brightening instead of quenching in acidic media). Ability to control sensor response direction is highly important to develop optimal sensors for targeted applications. The nanotubes' optical response to changes in solution pH is meaningful and provides new opportunities to develop optical pH sensors for wide applications including in healthcare, bioengineering, environmental sciences, and chemistry.

Received 28th June 2022,
Accepted 19th September 2022

DOI: 10.1039/d2sd00110a

rsc.li/sensors

Introduction

pH plays a significant role in chemical and biological processes. Changes in pH can be the cause or the result of diseases and malfunction in a biological system.[1] For example, several patho-physiological conditions such as tumor metastasis, microbial infection, blood glucose, female reproductive tract infections, and wound healing could cause changes in pH.[2–6] Thus, monitoring pH could provide insights on those patho-physiological changes. For instance, acidosis associated with bacterial colonization of the implant can be detected by pH changes on the surface of implanted medical devices.[2] Tumor tissues can be distinguished from normal tissues due to a lower pH (lysosomal pH in cancer cells; 3.8–4.7 and extracellular pH level in tumor environment; 6.2–6.9),[7–9] and its progression and growth may be followed by measuring the pH of the tumor fluid. The pH of an adults normal skin surface is acidic (pH 4.1–5.8), but disruption of the physical barrier leads to an increase of pH.[10] During wound healing, the pH of both acute and chronic wounds changes from basic to neutral to acidic.[11,12] Sweat pH changes can reveal information about atopic dermatitis, fungus infections, and cystic fibrosis (alkaline sweat up to pH 9).[13,14] Thus, sweat pH measurements could aid in accurately identifying certain health issues.

Solution pH can be measured by various methods including electrochemical, colorimetric, and fluorescence measurements.[1] System configuration of conventional electrochemical methods require a reference electrode and a wired system to measure pH changes. Despite high sensitivity under harsh environment, the need for a reference electrode

Department of Textile Engineering, Chemistry and Science, Wilson College of Textiles, North Carolina State University, Raleigh, NC, 27695, USA.
E-mail: jbudhat@ncsu.edu

† Electronic supplementary information (ESI) available: Photograph and additional plots. See DOI: https://doi.org/10.1039/d2sd00110a

and wired system increases the size posing challenges in their direct applications in biomedical uses.[15] Optical pH measurements have gained a significant interest in recent decades[16] due to versatile material choices and new imaging technologies that allow tuning the probes and sensors for exciting new applications including cell culture assays, *ex vivo*, and *in vivo* applications. In this regard, various classes of optical materials such as small molecule fluorophores and indicator dyes, polymers, metal–organic frameworks, and nanomaterials have been widely investigated for absorption- and luminescence-based pH sensors. While it is crucial to minimize photobleaching effects, fluorescence techniques employing common visible fluorophores (and fluorophore conjugated polymers and nanomaterials) frequently suffer from strong scattering, absorption, and autofluorescence, limiting penetration depth, and signal-to-noise ratios. Besides, pH indicators for use in biomedical applications perform better in the tissue transparent near infrared region where absorption, auto fluorescence and scattering from biological tissues and fluids are minimal.

Near infrared fluorophores are suitable candidates for optical pH indicators. Semiconducting single-walled carbon nanotubes (SWCNTs) have unique optical properties, which include an absorption at broader spectrum (UV-vis-nIR), bright fluorescence emission in the near-infrared spectral range (between 900 nm and 1600 nm), high sensitivity, high photostability, and longer lifetime.[17,18] Furthermore, SWCNTs' unique properties like their size, biocompatibility upon functionalization, high chemical, thermal, and mechanical stability, and ease of chemical functionalization, can enhance sensing performance in biosensor platforms.[19–22] Because of the ultra-low background and high penetration depths in biological tissues, this region of the electromagnetic spectrum (tissue transparency window) is advantageous for detection and bioimaging applications.[23–25] Therefore, with nIR emission, SWCNTs have an advantage in optical sensing and imaging.[25–27] The structural diversity of SWCNTs also allows for tunable emission wavelengths.[28,29] Thus, SWCNTs are considered valuable materials for developing sensors for various classes of analytes and can be utilized to perform environmental analysis, clinical analysis, and industrial analysis. Furthermore, photoluminescence on SWCNTs have been found sensitive towards pH changes and underlying mechanisms have been investigated in multiple studies.[30–34] Dukovic *et al.* used functionalized nanotubes, which showed photoluminescence (PL) quenching at low pH.[34] O'Connell *et al.* found that fluorescence of sodium dodecyl sulfate (SDS)-dispersed nanotubes quenched under acidic conditions.[30] The photoluminescence intensity was dramatically reduced by aggregation of the isolated nanotubes or by acidification of the SDS micellar suspension.[30] Strano *et al.* showed that an acidic pH caused fluorescence quenching and a basic pH restored the fluorescence reversibly.[32] Pre-adsorption of molecular oxygen, under ambient conditions, and sidewall protonation influenced the pH effects on nanotubes. Cognet *et al.* immobilized nanotubes dispersed in sodium dodecyl benzenesulfonate (SDBS) solution in agarose gel and reported pH-dependent reversible quenching of nanotube fluorescence by single-molecule reactions.[33] Carbon nanotubes that are non-covalently functionalized with DNA have also been investigated as potential optical pH sensors. Nißler *et al.* reported that non-covalently functionalized DNA-SWCNTs showed optical responses to pH changes induced by bacteria.[35] The study reported that $(GT)_{10}$-SWCNTs, responded to a pH drop from 7.4 to 4.3 by nanotube's intensity decrease. However, these DNA-SWCNTs showed lack of response to an increase in solution pH (pH 8.1). Thus, these nanotubes have limited scope where response to a wide pH range is required. Furthermore, some limitations of using DNAs as functionalizing molecules are that these biomolecules are prone to degradation under ambient conditions, difficult to synthesize, and cost prohibitive. Another approach for developing nanotube-based optical sensors include controlled covalent modification to induce defects on nanotubes and photoluminescence changes at the defect site. Kwon *et al.* showed that covalently functionalized/defect-induced nanotubes respond to pH changes through photoluminescence changes at the defect site.[36] Although this approach yielded sensitive optical probes towards pH changes, the method of functionalization is tedious and requires extensive time to develop sensors. A systematic investigation on developing a modular carbon nanotube-based optical pH sensor is still limited.

In this research, we used nIR fluorescent SWCNTs to construct optical sensor materials. We functionalized SWCNTs with pH-responsive amphiphilic compounds through a non-covalent method, resulting in dispersed nanotubes in aqueous solution. We showed that the nanotubes exhibit optical responses in the near-infrared region (900–1600 nm) under mild to high pH conditions, including pH range that is biologically relevant in disease conditions in a complex fluid such as artificial sweat as a model biofluid. Furthermore, these sensors respond to *in situ* pH changes. While previous studies on nanotube-based systems reported that nanotube's fluorescence in acidic solution is quenched, we showed that the sensor response direction can be tuned by modulating the nanotube's surface chemistry with a synthetic polymer (for example, brightening instead of quenching in acidic media) in complex solution (*e.g.*, model biofluid). Thus, the ability to control sensor response direction is highly important to develop optimal sensors for targeted applications.

Experimental section

Materials

Single-walled carbon nanotubes, (6,5) chirality, average diameter of ~0.78 nm diameter, ≥95% carbon basis (≥95% carbon nanotubes), sodium dodecyl benzenesulfonate (SDBS) and sodium dodecyl sulfate (SDS) (with a purity of >99%) were purchased from Sigma-Aldrich. Sodium cholate (SC) with a purity of 99% was purchased from Alfa-Aesar, New Zealand. Poly(diallyldimethylammonium chloride) (PDADMAC) with

average Mw 200 000–350 000 and the concentration 20 wt% in water was obtained from Sigma-Aldrich, USA. Artificial sweat was purchased from Pickering Laboratories Inc. The pH buffers were prepared using buffer capsules/powder obtained from Micro Essential Laboratory Inc. The materials were directly used without further purification.

Dispersion of SWCNTs with anionic surfactants

SWCNTs were dispersed following the reported procedures with some modifications.[18,37] In brief, 1 mg of SWCNTs was suspended in 2% sodium dodecylbenzenesulfonate (SDBS) solution and sonicated (Sonicator-FB505110, Fisherbrand Model 505 Sonic Dismembrator) for 30 min at an amplitude of 20% at low temperature using a precooled CoolRack (stored at −20 °C) and an ice bath. The sample was centrifuged (Centrifuge-75002436, Thermo Scientific™ Sorvall™ Legend™ Micro 21 Microcentrifuge) for 30 minutes, at 14 000 RPM at room temperature. Upon centrifugation, the residue, which mostly contains carbonaceous impurities and unsuspended nanotubes, was discarded and the supernatant was collected and re-centrifuged under the same conditions. The supernatant was diluted with deionized water for characterization by ultraviolet-visible-near-infrared (UV-vis-nIR) absorbance and fluorescence spectroscopies. Similar procedures were followed to disperse SWCNTs with sodium dodecyl sulfate (SDS) and sodium cholate (SC) separately. All experiments were performed at least in triplicate.

Characterization of surfactants–SWCNTs

The nanotube complexes were characterized by UV-vis-nIR absorbance and fluorescence spectroscopies. Near infrared fluorescence measurements were performed on NS-MiniTracer (NanoSpectralyzer from Applied NanoFluorescence LLC). A typical condition, 3000 ms integration, 3 averaging, for fluorescence was used for all measurements. Emission from 950 nm to 1350 nm was recorded and the data were directly exported from NS-MiniTracer. These data were analyzed and plotted using Microsoft Excel. UV-vis-NIR absorbance measurements were performed using a UV-vis-NIR spectrophotometer (Cary 5000 UV-vis-NIR spectrophotometer, Agilent Technologies, Inc.).

Preparation and characterization of SWCNTs complexes at varied pH

SWCNT suspensions at various pH ranges were prepared by using buffer capsules (Hydrion Buffer Capsules, Micro Essential Laboratory, Inc. USA). The solution pH was further determined by using a portable pH meter (Orion Star 221, ThermoFisher Scientific). The nIR fluorescence from the samples were compared to their respective controls. Near infrared fluorescence measurements were performed on NS-MiniTracer (NanoSpectralyzer from Applied NanoFluorescence LLC). Emission from 950 nm to 1350 nm was recorded and the data were directly exported from NS-MiniTracer. These data were analyzed and plotted using Microsoft Excel and GraphPad Prism. UV-vis-nIR absorbance measurements were performed in a UV-vis-NIR spectrophotometer (Cary 5000 UV-vis-NIR spectrophotometer, Agilent Technologies, Inc.).

Polymer addition to surfactant–SWCNTs

Poly(diallyldimethylammonium chloride) (PDADMAC) with average Mw 200 000–350 000 and the concentration 20 wt% in water was used. A 2% solution (weight/volume) of PDADMAC was prepared by diluting 20% PDADMAC aqueous solution in DI water. 100 μl of 2% diluted PDADMAC solution was added to each 400 μl solution of surfactant–SWCNTs complexes separately. SWCNT suspensions at various pH ranges were prepared by using buffer (Hydrion Buffer Capsules, Micro Essential Laboratory, Inc. USA). The solution pH was further determined by using a portable pH meter (Orion Star 221, ThermoFisher Scientific). Hereafter, near infrared fluorescence measurements were performed and emission from 950 nm to 1350 nm was recorded to generate the data being analyzed and plotted using Microsoft Excel and GraphPad Prism software.

Data analysis. All analysis were performed with GraphPad Prism software (GraphPad Software, CA). Statistical analysis was conducted *via* two-way ANOVA. Statistical significance was determined by p values. The p values which are less than 0.001 are summarized with three asterisks (***), and p values less than 0.0001 are summarized with four asterisks (****) on the bar graph. Simple regression analysis was run to get the trend line from each triplicating sample mean and average and its corresponding control mean and average.

Results and discussion

In this research, we used three anionic surfactants to disperse nanotubes in water. Fig. S1† includes chemical structures of the three surfactants – sodium dodecyl sulfate (SDS), sodium dodecyl benzene sulfonate (SDBS), and sodium cholate (SC) used to disperse SWCNTs in aqueous solution and Fig. 1a represents schematics for dispersion of nanotubes. SWCNTs are hydrophobic and remain in rope or bundle form due to the strong van der Waals force and π–π stacking interactions.[38,39] In this state, photoluminescence of SWCNTs remains quenched and does not show significant optical properties.[30] However, de-bundled SWCNTs obtained through non-covalent interactions with surfactants and polymers exhibit photoluminescence.[30] Amphiphilic compounds have been widely used to suspend SWCNTs in water due to high stability, efficiency, selectivity, and scalability.[40,41] As amphiphilic molecules percolate through the bundled SWCNTs, the hydrophobic parts of these molecules adsorb onto the wall of SWCNTs splitting the bundle apart.[38,39]

To obtain aqueous dispersion of nanotubes, a mixture of SWCNT powder and aqueous solution of a select dispersant was sonicated. The resulting dark aqueous suspension was centrifuged to remove any residue, which contains carbonaceous impurities, bundled structures and residual catalysts. The supernatant was characterized by UV-vis-nIR

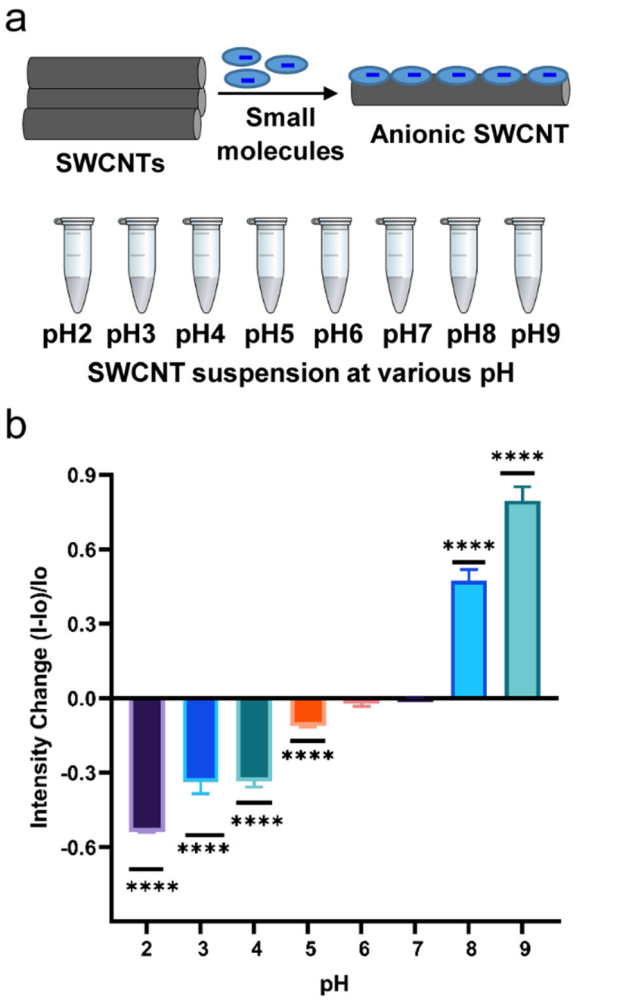

Fig. 1 Optical responses from SDBS-SWCNTs at various pH ranges. a) Schematic illustration of the process and nanotube suspension at various pH. b) Emission intensity change in response to pH, n = 3.

absorbance (Fig. S1a†) and nIR fluorescence (Fig. S1b†) measurements. The aqueous suspensions of SDS-SWCNTs, SDBS-SWCNTs and SC-SWCNTs were stable without visual aggregates for a few months.

The fluorescence from the surfactant–SWCNTs suspension appear to be dispersant-dependent. Our results show that among aqueous dispersion of SDBS-, SC-, and SDS-SWCNTs, SC-SWCNTs exhibited the highest emission intensity, followed by SDBS-SWCNTs and SDS-SWCNTs under similar experimental set-ups (Fig. S1c†). The differences can be explained based on specific molecular interactions between a surfactant and the nanotube due to differences in chemical identity of the surfactant molecule. Such molecular interactions result in various degrees of SWCNT surface coverage, exposure to solvent molecules, and dielectric environment. SC has a stiff amphiphilic structure with a steroid ring that is quasiplanar, somewhat curved, and rigid, with a hydrophilic face (the hydroxyl groups and the charged carboxylate group) and a hydrophobic face (the methyl groups and the tetracyclic carbon backbone) that are back-to-back.[42] Due to the slightly bent but stiff steroid ring in SC, it is expected that these surfactants can accommodate the curvature of the SWCNTs surface, hence improving the dispersion stability of SWCNTs in aqueous solutions.[43] SDBS, due to the planar aromatic structure, aligns parallel to the SWCNT surface to maximize aromatic π–π stacking.[44] SDS is a non-aromatic surfactant. We speculate that these differences in molecular interactions between surfactant and carbon nanotube cause differences in fluorescence intensity among SC-, SDBS-, and SDS-SWCNTs.

Nanotube's optical responses to solution pH

Anionic nanotube complexes (SDBS-SWCNTs, SDS-SWCNTs, and SC-SWCNTs) were exposed to acidic, basic, and neutral pH conditions and the optical responses at solution pH 2 to pH 9 were measured. In the acidic environment, the fluorescence was quenched (Fig. 1b and S2a†) in comparison to the respective controls for which the solution was maintained at pH 7. As seen in Fig. 1b for SDBS-SWCNTs, fluorescence intensity decreased by 54%, 34%, 33%, 12%, and 1.9% at pH 2, pH 3, pH 4, pH 5 and pH 6 respectively, compared to their respective controls at neutral pH. The results were significant compared to the controls. Fig. S2c† shows a pH response curve for the optical responses from SDBS-SWCNTs. Whereas SDS-SWCNTs showed about 65% and 23% decrease in nIR emission intensity at pH 2 and pH 4 respectively (Fig. S2a†). The overall quenching effects upon acid doping on surfactant–SWCNT suspensions observed in this study are consistent to previous reports[30–33] in which such fluorescence quenching on SDS- and SDBS-suspended nanotubes in acidic media was attributed to selective protonation of pre-adsorbed oxygen at the nanotube sidewalls. It is noteworthy that solution pH influences the solubility of the surfactant molecules through ionization because of protonation (at pH $<$ pK_a) and deprotonation (at pH $>$ pK_a) of the functional groups on the surfactants. As the solution pH becomes acidic, the anionic surfactant–SWCNTs experience various degrees of protonation. Furthermore, acidic pH can destabilize micelle structures[45,46] and induce reorganization of surfactant molecules on nanotube surface, which could provide a path through which the acid can reach the nanotube surface and quench the fluorescence. The pK_a values of dodecyl sulfuric acid, cholic acid, and *p*-dodecylbenzenesulfonic acid are 1.9, 4.98,[47,48] and 0.7 (estimated)[49] respectively. Thus, SC is protonated at pH $\leq$ 4, which reduces its ionization and water solubility. In fact, we observed aggregation of SC-SWCNTs at pH $\leq$ 4 (Fig. S3†).

When the pH of nanotube solution was tuned to a basic region (pH $>$ 7), nanotube photoluminescence was enhanced (Fig. 1b and S2a and b†). SDBS-SWCNTs exhibited significant emission changes about 48% and 81% increase in the emission intensity at pH 8 and pH 9 respectively (Fig. 1b). SDS-SWCNTs showed about 125% and 84% increase in emission intensity at pH 8 and pH 10, respectively. SC-SWCNTs showed 282% and 79% increase in emission

intensity at pH 8 and pH 10 respectively (Fig. S2b†). The results can be explained based on previously reported reversible sidewall protonation of carbon nanotubes, which may result in pH-sensitive fluorescence modulation.

Nanotube's optical responses to *in situ* pH changes

In many instances, it is crucial to report *in situ* pH changes (acidic to basic and *vice versa*). We investigated the optical responses from the nanotubes upon *in situ* pH changes from neutral to an acidic pH followed by a basic pH in a sequence of events (steps 1–2, Fig. S4a†). First, the pH of the nanotube solution was changed from neutral to an acidic pH (pH 4, step 1, Fig. S4a†) and the optical responses were recorded. The solution pH of the nanotube suspension was then changed to pH 8 (step 2, Fig. S4a†). The optical responses were recorded upon changes in solution pH at each step. The pH adjustments were made by adding pH buffers to nanotube suspension and the DI water in controls to compensate for dilution effects. The solution pH was confirmed by using a pH meter before and after the optical measurements. Fig. S4(b and c)† show that both SDBS-SWCNTs and SDS-SWCNTs exhibited fluorescence quenching at pH 4. Changes in the solution pH from pH 4 to pH 8 was accompanied by fluorescence intensity enhancement as compared to respective controls at neutral pH. Thus, the nanotubes once quenched under acidic conditions can be de-quenched through pH modulation. The results are consistent to previous reports in which the fluorescence was restored in pre-acid treated nanotubes either by adding alkaline solution or by degassing the solution to remove adsorbed oxygen.[30–32,50] The effects can be attributed to reversible sidewall protonation that localizes valence electrons, quenching the nanotube's fluorescence emission.[30] The responses from the nanotubes under these sequential (*in situ*) pH changes (Fig. S4†) were consistent to responses at specified individual pH conditions (Fig. 1b and S2†), albeit the degree of changes were comparatively smaller in acid-pretreated nanotubes. These responses also indicate that acidic and basic environments do not cause a permanent effect on these nanotubes. With similar responses from both SDS- and SDBS-SWCNT systems towards pH changes, we chose SDBS-SWCNTs as a model system for kinetics measurements.

Kinetics measurements on SDBS-SWCNT's optical responses

For applications, it is important to establish that the indicator response is measurable within a defined period. To determine the nanotube's response to specified pH, we performed kinetics measurements on SDBS-SWCNTs system responding to a specified solution pH. The fluorescence from SDBS-SWCNTs was measured at pH 8 at 5-minute intervals up to 90 minutes. As shown in Fig. 2, fluorescence intensity increased up to the first 65 minutes and then plateaued for the remaining time (*ca.* 90 minutes). Furthermore, a considerable response even within first 5–10 minutes of

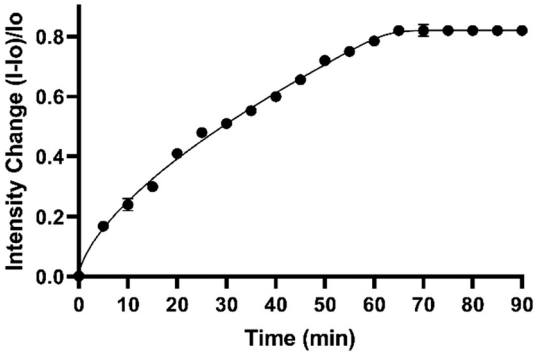

Fig. 2 Kinetics measurements of intensity changes of SDBS-SWCNTs over time at pH 8.

treatment makes these nanotubes promising materials for sensor development.

Surface chemistry modulation on anionic–SWCNTs and the optical responses to pH changes

In the previous section, the optical responses of anionic surfactant–SWCNTs to a change in solution pH (2–10) has been discussed. The nanotubes responded to basic pH (8–10) *via* fluorescence enhancements and to acidic pH ranges (2–5) *via* fluorescence quenching. In many situations, it is important to collect signals under acidic conditions. For instance, in acidosis and tumor metathesis, biological tissues experience a pH drop. Due to quenching effects, the nanotube's optical signal in the acidic pH ranges (2–6) gets weaker, potentially causing a low sensitivity from turn-off signals. A probe with 'turn on' response could mitigate such issues.

Surface chemistry can modulate the photoluminescence of nanotubes.[30,51] We modulated the surface chemistry on SDBS- and SDS-SWCNTs by introducing a cationic polymer to trigger electrostatic interactions between nanotube's anionic surface coating and the cationic polymer. This electrostatic interaction neutralizes excessive negative charges on nanotube adsorbents. We hypothesized that the charge modulation on the anionic nanotubes could produce an opposite optical response to specified pH as new chemistry could affect nanotubes sidewall protonation, a phenomenon that has been shown to influence nanotube photoluminescence under acidic pH environment. Experimentally, a cationic polymer could be added onto the anionic surfactant–SWCNTs to modulate the nanotube's surface chemistry. We used a cationic polyelectrolyte, poly(diallyldimethylammonium chloride) (PDADMAC), which is widely used to bind to anionic molecules through electrostatic interactions.[52] Addition of the positively charged polymer (PDADMAC) to an anionic surfactant–nanotube system triggers changes in molecular adsorption characteristics onto the surface of the carbon nanotubes due to a strong electrostatic interaction between oppositely charged molecules on the nanotube surface. Both pH and ionic strength can influence the electrostatic interaction between the oppositely charged

molecules.[53] Ionic strength affects the properties of electrostatic complexes due to charge screening, whereas pH can modulate the degree of charges on polyelectrolytes. For weak electrolytes, ionization extent is controlled by solution pH and ionic strength, which makes the electrostatic complexations in weak polyelectrolytes responsive to external variations. On the other hand, for strong electrostatic complexation, associative complexes are spontaneously formed. With surfactant-suspended nanotubes, addition of a strong polyelectrolyte polymer, PDADMAC, most likely results in spontaneous complexation that could remain stable under moderate conditions of ionic strength and pH changes. We introduced PDADMAC polymer solution into SDBS-SWCNT suspension (Fig. 3a). The PDADMAC–SDBS-SWCNTs were then subjected to various pH conditions and the optical responses from the nanotubes were measured. Interestingly, we found that the addition of PDADMAC to SDBS-SWCNTs made the nanotubes respond to an acidic pH with an enhanced emission intensity up to 97% and to a basic pH with quenching effects down to 40% with significant signal changes except for pH 6 (Fig. 3b). The fluorescence intensity increased by 97%, 70%, 60%, 11%, and 1.9% at pH values 2, 3, 4, 5, and 6 respectively compared to their respective control at neutral pH. The nanotubes responded to basic solution pH with a decrease in fluorescence intensity with 40% and 27% at pH values 9 and 8 respectively. The results showed a linear trend with a goodness of fit 95%. Results from SDS-SWCNTs showed a similar trend with emission intensity increased at pH 4 and intensity decreased at pH 8 (Fig. S5†). These results, upon addition of cationic polymer to anionic nanotubes, were in the opposite trend as compared to results from anionic SDBS-SWCNTs in the absence of PDADMAC polymer (Fig. 1b). The electrostatic interactions between the PDADMAC and anionic surfactants–SWCNTs could disrupt adsorption of surfactants on nanotubes and perturb surface charges influencing the sidewall protonation and the excitonic behaviors on nanotubes. Furthermore, this interaction could also influence oxygen adsorption, hydration, and nanotube's exposure to polar solvent molecules, all of which can affect the photoluminescence.

We then further studied the modified nanotubes' response to *in situ* pH changes from neutral to acidic and then to basic region. Under this condition, PDADMAC–SDS-SWCNTs were evaluated for their responses at acidic and basic pH. Fig. S5e† shows that the nanotubes responded to an acidic pH (pH 4) with fluorescence intensity enhancement by 19% and to a basic pH (pH 8) with decrease in emission intensity by 16%.

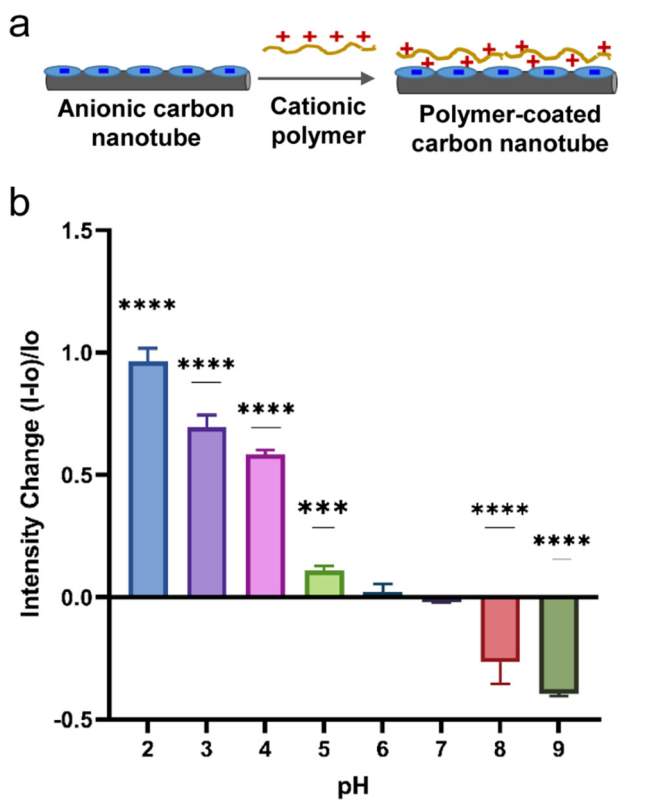

Fig. 3 Surface chemistry modulation on nanotubes and optical responses at various pH. a) Schematic illustration of surface chemistry modulation. b) Intensity changes of PDADMAC–SDBS-SWCNTs in response to solution pH changes, n = 3.

Optical response in artificial sweat

For practical applications, the probes and sensors should retain their responses in a complex environment. This is important because biofluids, tissues, and other biological samples are complex and the molecular probes/sensors will experience a complex environment. We investigated whether the nanotubes could respond to specific pH in a complex aqueous system. We used artificial sweat as a model biofluid to evaluate the performance of these pH-sensitive nanotubes in a complex system.

We first used nanotubes without polymer coatings (*e.g.*; SDBS-SWCNTs and SDS-SWCNTs) to evaluate the responses. Following the similar procedure described previously, SDBS-SWCNTs and SDS-SWCNTs were exposed to artificial sweat at acidic and basic pH conditions (Fig. S6a†) and the optical responses at pH 2 to pH 10 were measured. Artificial sweat at pH 5.5 and pH 8 were used as received. Further pH modulation was achieved by adding buffer and a few drops of either dilute hydrochloric acid or dilute sodium hydroxide solution as needed. The solution pH remained stable throughout the experiments as confirmed by a pH meter. All these anionic surfactant–SWCNTs complexes showed emission intensity enhancement in the basic environment (pH 8–10). In the acidic environment, the emission intensity was quenched for all surfactant–SWCNTs in comparison to the controls for which solution was neutral at pH 7 (Fig. S6b†).

SDBS-SWCNTs showed around 65% and 17% decrease in the emission intensity at pH 2 and pH 5.5 respectively (Fig. S6b†); whereas SDS-SWCNTs showed 30% and 38% decrease in nIR emission intensity at pH 2 and pH 5.5 respectively (Fig. S6b†). Likewise, nIR emission intensity increased by about 107% and 114%, respectively, at pH 8 and pH 10 for SDBS-SWCNTs (Fig. S6b†). For SDS-SWCNTs, the emission

intensity increased by 62% and 60% at pH 8 and 10, respectively (Fig. S6b†). Similarly, for SDBS-SWCNT sequential test *in situ*, the emission intensity decreased by about 55% at pH 4 (Fig. S6d†). Modulating the solution pH to pH 8 increased the intensity by 17%, and finally modulating the solution pH from pH 8 to pH 4 again (represented as pH4r in Fig. S6d†) decreased the emission intensity by about 61% (Fig. S6d†). In parallel, the sequential pH changes experiment for SDS-SWCNT, intensity decreased by 57% at pH 4, then increased by 20% at pH 8, and again in acidic pH (pH 4), the intensity decreased by about 30% as shown in Fig. S6d.†

With these consistent and predictable results in artificial sweat samples, we then further investigated whether modulating the nanotube's surface chemistry could control the optical response direction under acidic and basic conditions. As described previously, a positively charged polymer (PDADMAC) was added to the anionic surfactant dispersed SWCNTs to modulate the nanotube's surface chemistry (Fig. 4a). The modified PDADMAC–SDBS-SWCNTs were then added into artificial sweat at specified pH. PDADMAC–SDBS-SWCNTs were tested from pH 2–9 at an interval of 1 unit to cover a wide range of pH scale. Fig. 4b shows that these nanotubes responded to acidic sweat by increased emission intensity up to 107% and to basic sweat by reduced emission down to 63%. The fluorescence intensity increased by 107%, 102%, 81%, 41%, and 7% at pH values 2, 3, 4, 5 and 6, respectively as compared to their respective controls at neutral pH. These results were significant for both acidic and basic pH range. In biochemical processes, pH changes occur in small increments prior to reaching to their extreme values. Therefore, we evaluated the optical responses from the nanotubes at an interval of 0.5 pH units within a narrow acidic pH range (pH 2–4.5). The results showed that PDADMAC–SDBS-SWCNTs could differentiate these narrow pH intervals with pH dependent significant emission changes (Fig. S7†). As sweat contains various electrolytes including sodium and chloride, a sweat sensor should be able to function in salt-rich environment. Therefore, we evaluated the nanotubes' response to pH in the artificial sweat at pH 5 with increasing concentration of sodium chloride (50 mM, 100 mM, 150 mM, 200 mM, 300 mM). Our results showed that addition of salt at these concentrations did not cause any significant changes in the optical response. These results in artificial sweat suggests that these carbon nanotube-based materials are compelling candidates for further development of optical pH detection systems.

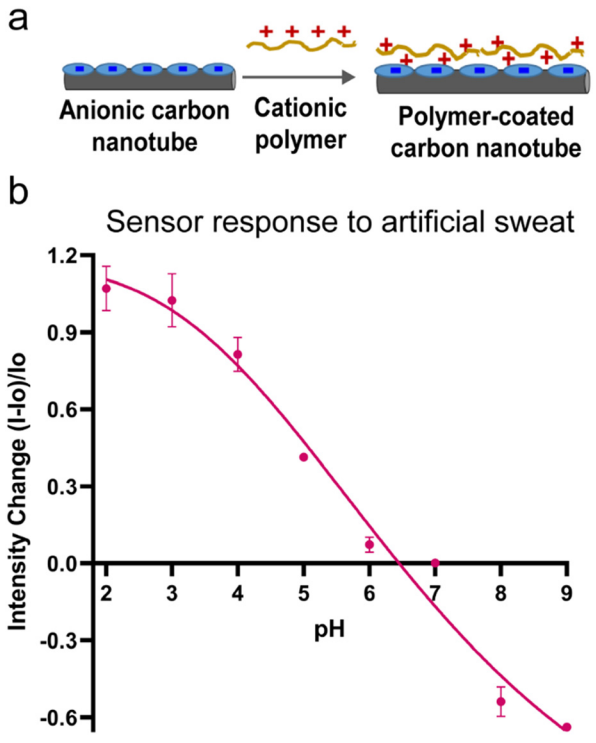

Fig. 4 Optical responses from PDADMAC–SDBS-SWCNTs in artificial sweat at acidic and basic pH. a) Schematic illustration of the nanotube complex. b) pH response curve showing intensity changes at specified pH. The solid line represents linear regression fits, $n = 3$.

Conclusions

We have reported pH responsive nanotube complexes, which enable optical detection of pH changes in a wide pH range in complex solution such as artificial sweat. Two different types of non-covalent functionalization approaches were employed to develop optical nanosensors – small molecules adsorbed on SWCNTs and their further functionalization with polymer deposition. Both systems exhibited optical response to a wide pH range, which is relevant in biology, biochemical processes, and industrial processes. We also showed that the optical response could be modulated *via* modulation of the nanotube's surface chemistry. Although other methods of functionalization including defect-induced covalent functionalization approach and DNA-SWCNTs have been investigated to measure pH changes, the current approach of non-covalent functionalization using small molecules and polymers provides a more straight-forward, versatile, and efficient route to develop nanotube-based sensors. The results suggest that functionalized carbon nanotubes provide a basis for sensor materials towards the development of optical pH sensors for biofluids analysis. As carbon nanotubes can be integrated into various form factors including biocompatible gels, polymeric scaffolds, paints, fibers, *etc.*, the findings from the current research provides new opportunities in developing new optical sensor platforms for exciting new opportunities in biomedical applications. More importantly, the study demonstrated that the sensor response direction can be tuned and the sensor has potential for bodily fluids analysis. Future investigation is warranted for developing the solid/gel or patch form of these sensors for practical purposes. We expect this work to be a valuable tool in biomedical sciences where very tiny sensor need to be implanted or can be used for *in vitro* analysis, which may reduce invasive techniques for biological pH measurements.

Author contributions

N. S.: investigation, methodology, validation, analysis, data curation, and writing original draft; H. D.: resources, writing review and editing; J. B. U.: conceptualization, supervision, writing review and editing, funding acquisition, and resources. The manuscript was written through contributions of all authors. All authors have given approval to the final version of the manuscript.

Conflicts of interest

The authors declare no competing financial interest.

Acknowledgements

The authors acknowledge funding support from Textile Engineering, Chemistry and Science Department, North Carolina State University through new faculty startup funds. The authors thank Jaron Jones, Graham Neve, and Julia Drago for their assistance with preliminary experimentation, Meghan Lord for helpful discussion, Dr. Jialong Shen and Dr. Sonja Salmon for assistance with pH meter, and Ms. Birgit Andersen for assistance in using Cary 5000 UV-vis-NIR spectrophotometer, Agilent Technologies, Inc.

References

1 M. T. Ghoneim, *et al.*, Recent Progress in Electrochemical pH-Sensing Materials and Configurations for Biomedical Applications, *Chem. Rev.*, 2019, **119**, 5248–5297.
2 L. Wang, *et al.*, Imaging acidosis in tumors using a pH-activated near-infrared fluorescence probe, *Chem. Commun.*, 2012, **48**, 11677–11679.
3 S. Schreml, *et al.*, The impact of the pH value on skin integrity and cutaneous wound healing, *J. Eur. Acad. Dermatol. Venereol.*, 2010, **24**, 373–378.
4 K. Y. B. Ng, *et al.*, In vivo oxygen, temperature and pH dynamics in the female reproductive tract and their importance in human conception: A systematic review, *Hum. Reprod. Update*, 2018, **24**, 15–34.
5 F. Rippke, E. Berardesca and T. M. Weber, pH and Microbial Infections, *Curr. Probl. Dermatol.*, 2018, **54**, 87–94.
6 X. Strakosas, *et al.*, A non-enzymatic glucose sensor enabled by bioelectronic pH control, *Sci. Rep.*, 2019, **9**, 10844–10847.
7 M. Y. Mboge, *et al.*, Carbonic Anhydrases: Role in pH Control and Cancer, *Metabolites*, 2018, **8**, 19.
8 A. I. Hashim, *et al.*, Imaging pH and metastasis, *NMR Biomed.*, 2011, **24**, 582–591.
9 S. Siriwibool, *et al.*, Near-Infrared Fluorescent pH Responsive Probe for Targeted Photodynamic Cancer Therapy, *Sci. Rep.*, 2020, **10**, 1283.
10 E. Proksch, pH in nature, humans and skin, *J. Dermatol.*, 2018, **45**, 1044–1052.
11 W. Slone, *et al.*, The Effect of pH on the Antimicrobial Efficiency of Silver Alginate on Chronic Wound Isolates, *J. Am. Coll. Clin. Wound Spec.*, 2010, **2**, 86–90.
12 L. A. Wallace, L. Gwynne and T. Jenkins, Challenges and opportunities of pH in chronic wounds, *Ther. Delivery*, 2019, **10**, 719–735.
13 W. Dang, *et al.*, Stretchable wireless system for sweat pH monitoring, *Biosens. Bioelectron.*, 2018, **107**, 192–202.
14 Y. S. Oh, Skin-Attachable, Stretchable Electrochemical Sweat Sensor for Glucose and pH Detection, *ACS Appl. Mater. Interfaces*, 2018, **10**, 13729–13740.
15 H. Y. Y. Nyein, A Wearable Electrochemical Platform for Noninvasive Simultaneous Monitoring of Ca^{2+} and pH, *ACS Nano*, 2016, **10**, 7216–7224.
16 D. Wencel, T. Abel and C. McDonagh, Optical Chemical pH Sensors, *Anal. Chem.*, 2014, **86**, 15–29.
17 A. Jain, *et al.*, Single-walled carbon nanotubes as near-infrared optical biosensors for life sciences and biomedicine, *Biotechnol. J.*, 2015, **10**, 447–459.
18 M. S. Strano, *et al.*, Near-infrared optical sensors based on single-walled carbon nanotubes, *Nat. Mater.*, 2005, **4**, 86–92.
19 J. Ackermann, *et al.*, Biosensing with Fluorescent Carbon Nanotubes, *Angew. Chem., Int. Ed.*, 2022, **61**, e202112372.
20 A. Hendler-Neumark and G. Bisker, Fluorescent Single-Walled Carbon Nanotubes for Protein Detection, *Sensors*, 2019, **19**, 5403.
21 M. M. Safaee, M. Gravely and D. Roxbury, A Wearable Optical Microfibrous Biomaterial with Encapsulated Nanosensors Enables Wireless Monitoring of Oxidative Stress, *Adv. Funct. Mater.*, 2021, **31**, 2006254.
22 R. M. Williams, *et al.*, Glutathione-S-transferase Fusion Protein Nanosensor, *Nano Lett.*, 2020, **20**, 7287–7295.
23 J. P. Giraldo, *et al.*, A Ratiometric Sensor Using Single Chirality Near-Infrared Fluorescent Carbon Nanotubes: Application to In Vivo Monitoring, *Small*, 2015, **11**, 3973–3984.
24 H. Yi, *et al.*, M13 Phage-Functionalized Single-Walled Carbon Nanotubes as Nanoprobes for Second Near-Infrared Window Fluorescence Imaging of Targeted Tumors, *Nano Lett.*, 2012, **12**, 1176–1183.
25 J. Pan, F. Li and J. H. Choi, Single-walled carbon nanotubes as optical probes for bio-sensing and imaging, *J. Mater. Chem. B*, 2017, **5**, 6511–6522.
26 M. Zheng, *et al.*, DNA-assisted dispersion and separation of carbon nanotubes, *Nat. Mater.*, 2003, **2**, 338–342.
27 S. F. Oliveira, *et al.*, Protein functionalized carbon nanomaterials for biomedical applications, *Carbon*, 2015, **95**, 767–779.
28 S. Kruss, *et al.*, Carbon nanotubes as optical biomedical sensors, *Adv. Drug Delivery Rev.*, 2013, **65**, 1933–1950.
29 S. M. Bachilo, *et al.*, Structure-Assigned Optical Spectra of Single-Walled Carbon Nanotubes, *Science*, 2002, **298**, 2361–2366.
30 M. J. O'Connell, *et al.*, Band Gap Fluorescence from Individual Single-Walled Carbon Nanotubes, *Science*, 2002, **297**, 593–596.
31 J. G. Duque, *et al.*, Stable Luminescence from Individual Carbon Nanotubes in Acidic, Basic, and Biological Environments, *J. Am. Chem. Soc.*, 2008, **130**, 2626–2633.

32 M. S. Strano, *et al.*, Reversible, Band-Gap-Selective Protonation of Single-Walled Carbon Nanotubes in Solution, *J. Phys. Chem. B*, 2003, **107**, 6979–6985.
33 L. Cognet, *et al.*, Stepwise Quenching of Exciton Fluorescence in Carbon Nanotubes by Single-Molecule Reactions, *Science*, 2007, **316**, 1465–1468.
34 G. Dukovic, *et al.*, Reversible Surface Oxidation and Efficient Luminescence Quenching in Semiconductor Single-Wall Carbon Nanotubes, *J. Am. Chem. Soc.*, 2004, **126**, 15269–15276.
35 R. Nißler, *et al.*, Remote near infrared identification of pathogens with multiplexed nanosensors, *Nat. Commun.*, 2020, **11**, 5995.
36 H. Kwon, *et al.*, Optical Probing of Local pH and Temperature in Complex Fluids with Covalently Functionalized, Semiconducting Carbon Nanotubes, *J. Phys. Chem. C*, 2015, **119**, 3733–3739.
37 D. A. Heller, *et al.*, Optical Detection of DNA Conformational Polymorphism on Single-Walled Carbon Nanotubes, *Science*, 2006, **311**, 508–511.
38 H. Cui, *et al.*, Effects of Various Surfactants on the Dispersion of MWCNTs–OH in Aqueous Solution, *Nanomaterials*, 2017, **7**, 262.
39 M. López-López, *et al.*, Study of ionic surfactants interactions with carboxylated single-walled carbon nanotubes by using ion-selective electrodes, *Electrochem. Commun.*, 2016, **67**, 31–34.
40 R. Haggenmueller, *et al.*, Comparison of the Quality of Aqueous Dispersions of Single Wall Carbon Nanotubes Using Surfactants and Biomolecules, *Langmuir*, 2008, **24**, 5070–5078.
41 J. N. Coleman, Liquid-Phase Exfoliation of Nanotubes and Graphene, *Adv. Funct. Mater.*, 2009, **19**, 3680–3695.
42 L. B. Pártay, P. Jedlovszky and M. Sega, Molecular Aggregates in Aqueous Solutions of Bile Acid Salts. Molecular Dynamics Simulation Study, *J. Phys. Chem. B*, 2007, **111**, 9886–9896.
43 M. S. Arnold, *et al.*, Hydrodynamic Characterization of Surfactant Encapsulated Carbon Nanotubes Using an Analytical Ultracentrifuge, *ACS Nano*, 2008, **2**, 2291–2300.
44 C. F. Chiu, *et al.*, Defect-Induced Near-Infrared Photoluminescence of Single-Walled Carbon Nanotubes Treated with Polyunsaturated Fatty Acids, *J. Am. Chem. Soc.*, 2017, **139**, 4859–4865.
45 H. Lu, *et al.*, pH-regulated surface properties and pH-reversible micelle transition of a zwitterionic gemini surfactant in aqueous solution, *Phys. Chem. Chem. Phys.*, 2016, **18**, 32192–32197.
46 L. Wasungu, *et al.*, Transfection mediated by pH-sensitive sugar-based gemini surfactants; potential for in vivo gene therapy applications, *J. Mol. Med.*, 2006, **84**, 774–784.
47 H. Li and L. Zhou, Visualizing Helical Wrapping of Semiconducting Single-Walled Carbon Nanotubes by Surfactants and Their Impacts on Electronic Properties, *ChemistrySelect*, 2016, **1**, 3569–3572.
48 Cholic Acid, Drugbank Online, **https://www.drugbank.ca/drugs/DB02659/**, (accessed June 17, 2022).
49 A. T. Tran, *et al.*, Proton transfer and esterification reactions in EMIMOAc-based acidic ionic liquids, *RSC Adv.*, 2017, **7**, 18333–18339.
50 D. Wang and L. Chen, Temperature and pH-Responsive Single-Walled Carbon Nanotube Dispersions, *Nano Lett.*, 2007, **7**, 1480–1484.
51 J. Budhathoki-Uprety, *et al.*, Helical Polycarbodiimide Cloaking of Carbon Nanotubes Enables Inter-Nanotube Exciton Energy Transfer Modulation, *J. Am. Chem. Soc.*, 2014, **136**, 15545–15550.
52 L. Patel, *et al.*, Interaction of Low Molecular Weight Poly(diallyldimethylammonium chloride) and Sodium Dodecyl Sulfate in Low Surfactant–Polyelectrolyte Ratio, Salt-Free Solutions, *Langmuir*, 2020, **36**, 8815–8825.
53 C. G. Otoni, *et al.*, Charge Matters: Electrostatic Complexation as a Green Approach to Assemble Advanced Functional Materials, *ACS Omega*, 2020, **5**, 1296–1304.